

Assessing and benchmarking the performance of advanced façades

Chapter 24 in *Materials for Energy Efficiency and Comfort in Buildings and*

***Occupied Spaces*, Hall, M, Ed., Woodhead Publishing Energy Series No. 14,**

ISBN: 1-84569-526-7

Clarke J A and Johnstone C M

Energy Systems Research Unit

University of Strathclyde

esru@strath.ac.uk

Content

Abstract

Keywords

Advanced façades

Façade component options

Performance models and model parameter measurement

Integrated performance rating

Application in practice

Benchmarking façade performance

Further information

References

Abstract

This chapter describes the energy demand reshaping and supply technologies that may be encapsulated within an advanced building façade – for example, transparent and

breathable insulation, advanced glazing, daylight capture, photovoltaic components and ducted wind turbines. Laboratory testing techniques for the characterisation of the fundamental parameters underlying each technology are elaborated as the essential prerequisite of integrated performance appraisals of specific technology combinations within an advanced façade design context. Based on the results from simulations undertaken in the UK climate context, performance benchmarks are suggested for some principal façade configurations.

Keywords: advanced façades, demand reduction, renewable supply, integrated performance assessment, performance benchmarks.

Advanced façades

In support of the deployment of urban-scale new and renewable energy systems, attention is being directed to the energy demand-supply interface within the urban context in an attempt to enhance the temporal match. Whatever approach is taken, it is likely that demand profile reshaping will be as important as overall demand reduction because the former can facilitate the integration of energy sources that are both intermittent and stochastic. Advanced façades (Selkowitz *et al* 2003, Façade Engineering 2009) can play a significant role in this regard because of the potential to blend technical systems that affect both energy demand and local supply. However, designers of such façades are then confronted by three significant issues: how to characterise the performance of specific technologies, how to evaluate the performance impacts when technologies are combined within a given façade, and how to judge the outcome in terms of overall cost-effectiveness. This chapter describes laboratory approaches that may be used to address the first issue, and an integrated

simulation approach that addresses the second issue and aspects of the third: the issue of cost is not addressed here. Examples of advanced façades that incorporate innovative components are then presented and performance data are extracted that may be used to benchmark advanced façade designs.

Façade component options

There are several existing technologies that may be integrated within an advanced façade and these can be conveniently categorised into those that reshape/reduce demand and those that supply energy from locally deployed heat and power generating components.

Demand reshaping

Several options exist to reshape/reduce energy demand. Basic insulation and capacity can be enhanced to an optimum level beyond which the law of diminishing returns will apply. Concepts such as breathable (Imbabi and Peacock 2004) and transparent (Wittwer and Platzer 2000) insulation can be deployed whereby heat loss reduction is enhanced: in the former case, by utilising the solar energy contained in the surface boundary layer; in the latter case, by allowing the deep transmission of the incident solar flux. Advanced glazings (Hutchins 1998) can be employed to change demand through switchable properties (thermo-, photo- and electro-chromic coatings), heat loss reduction (low emissivity coatings and low conductivity inter-pane gas), light redirection (prismatic coatings and attached light shelves) or integrated mechanical devices (shading devices and shutters). Double envelopes (Loncour *et al* 2004) can also be introduced to provide solar ventilation, air pre-heating and/or passive cooling in addition to lowered thermal transmission and daylight control.

Energy supply

Several technologies can be integrated within the façade to provide thermal and electrical energy from renewable sources. Photovoltaic cells (IEA 2002) can be deployed to convert the incident solar flux to electrical power and, where used in hybrid mode, to also produce heat (this mode of operation has the added advantage in the case of crystalline cells of reducing cell temperature and so maintaining optimum energy conversion efficiency). Advanced glazings can also be used to enhance/control the penetration of daylight to the interior; a photocell-based control system may then be deployed to regulate artificial lighting use in a complementary manner in order to displace the consumption of high grade electricity. Ducted wind turbines (Grant *et al* 2008) can be deployed at the roof junction to produce electrical power by reducing the pressure at the leeward side of the duct through the action of an integrated spoiler, thereby enhancing inward air flow at the windward side. Where a double façade is employed, the solar chimney effect can be used to enhance the air flow at turbine entry.

Just as the technology deployment options are many, so are the conflicts that can arise because of the interactions between technologies when deployed in various combinations. The core issue addressed in this chapter is ‘how can the multi-variate impacts of alternative deployment combinations be assessed at the design stage in order to inform decision-making that respects the implicit performance trade-offs?’ For example, will a photovoltaic façade harvesting renewable solar power to provide

electricity give rise to a more cost-effective solution than (mutually exclusive) daylight capture devices deployed as a means to reduce electricity usage?

Performance models and model parameter measurement

Building performance simulators operate in the transient domain based on models of material and component behaviour that require a range of fundamental parameters determined by experimental means. In order to facilitate integrated performance assessment and benchmarking, it is therefore necessary to decide on suitable prediction models and establish representative values for their related input parameters. For example, breathable insulation might be represented by a conduction model that employs an equivalent overall conductivity, which needs to be identified before the model can be used. Alternatively, a more refined model might be employed that differentiates between conductive and convective heat transfer and so requires values for the parameters relating to these distinct mechanisms. For complete systems, such as photovoltaic components, quoted performance is often related to a standard test condition and the underlying model serves to translate performance to the non-standard conditions encountered throughout a simulation. Models and experimental methods exist for each of the demand/supply technologies mentioned in the previous section and these are summarised here.

Material properties

The position of some materials within an advanced façade, such as insulation, will ensure that they operate in the dry state. For this case, the measurement of conductivity is carried out by either the guarded hot-plate or heat flow meter technique. The former has an accuracy of around $\pm 3\%$. The latter apparatus is simpler

to use but requires the availability of calibration samples measured by the hot-plate method so that the overall error may be around twice that of the hot-plate method.

Where a material operates in the moist state, the measurement of conductivity is problematic because the application of a temperature difference to a moist specimen results in a moisture gradient, causing moisture to migrate from the higher temperature. At constant applied temperature difference, the same sample will have different moisture gradients for different moisture contents while, at constant moisture content, the same sample will have different moisture gradients for different applied temperatures. Furthermore, as the moisture content increases, condensate will appear at the cold side of the specimen implying that the measured conductivity will increasingly fall below the conductivity for a linear moisture distribution with increasing moisture content. In the absence of knowledge of the moisture gradient, quoting applied temperatures at constant moisture content does not uniquely define the conductivity measurement. Instead, measurements become particular functions of temperature, moisture content, sample thickness, sample orientation (up- or downward heat flow) and length of measurement period. The thin-heater thermal conductivity apparatus uses a low applied temperature difference to reduce the problem of moisture migration.

With regard to specific heat capacity, the seemingly straightforward definition of this parameter as the amount of heat energy required to be added or removed to change unit weight of a material by unit temperature belies the difficulty of measurement. One difficulty, particularly for materials of low conductivity, is that it is difficult to input or extract heat quickly, making the design of accurate practical experimental

apparatus difficult. Test techniques include conventional absolute calorimetric methods and indirect dynamic methods based on Fourier's equation and regression analysis applied to test results.

Because of the high specific heat capacity of water, the effect of moisture content on the specific heat of a material is significant and must be taken into account. In principle, the overall specific heat capacity of a material is the linear addition of that of the dry material to that due to the amount of water present. In practice, this requires knowledge of the in-use moisture content. While calculations can be based on standard design values, the absence of a practical, non-destructive test method for determining on-site moisture content gives rise to an inherent uncertainty in calculating values of specific heat capacity for moisture containing materials. This uncertainty is compounded because it is the volume heat capacity (i.e. the product of density and specific heat capacity) that is important in determining thermal capacity; hence, the uncertainty in density is added to the uncertainty in specific heat capacity for volume heat capacity.

A further source of error will arise from the fact that conditions are dynamic in practice. In general, materials will be subject internally to temperature and moisture gradients that do not correspond to equilibrium distributions. Hence, both the thermal resistivity and capacity will vary within the material. It is also the case that the specific heat capacity is a function of temperature. Given the relatively small range of temperature involved in calculating the thermal performance of buildings, the error associated with adopting a single, steady-state value may be insignificant compared to the scale of error from other causes. Such an assumption would not be acceptable in

modelling applications where moisture dependent heat transfer dominates (Künzel and Kiessl 1997, Rode and Grau 2008). Chapters 5 and 16 give further information on the hygrothermal properties of materials, while hygrothermal property data are available in the literature (e.g. Kumaran 1996, Clarke and Yaneske 2009).

Other material properties required to support the integrated modelling process include opaque surface emissivity, absorptivity and reflectivity as required for radiation modelling within the longwave, shortwave and visible portions of the electromagnetic spectrum respectively.

Glazing materials have the added property of transmissivity in addition to those of reflectivity and absorptivity. As the sum of the three properties must equal unity, it is only necessary to measure two properties. Glazing manufacturers publish basic data on the solar optical properties of various forms of sheet glass and transparent plastic materials, and modelling systems are available that provide optical data as a function of flux angle of incidence and specific window configuration. (e.g. Window 5.2 available from <http://windows.lbl.gov/software/window>).

Transparent insulation

Transparent insulation (TI) allows solar energy to be transferred to an intra-façade location where a material of suitable thermal capacity is located and used to effect amplitude dampening and time delay. While the angular shortwave transmittance may be determined as above, a new issue arises: the possible degradation in performance where encapsulation is not air tight and penetrating air flow can deposit dust particles within the TI honeycomb structure resulting in surface staining. In this case, the

impact on angular shortwave transmissivity can be established experimentally as shown in Figure 1.

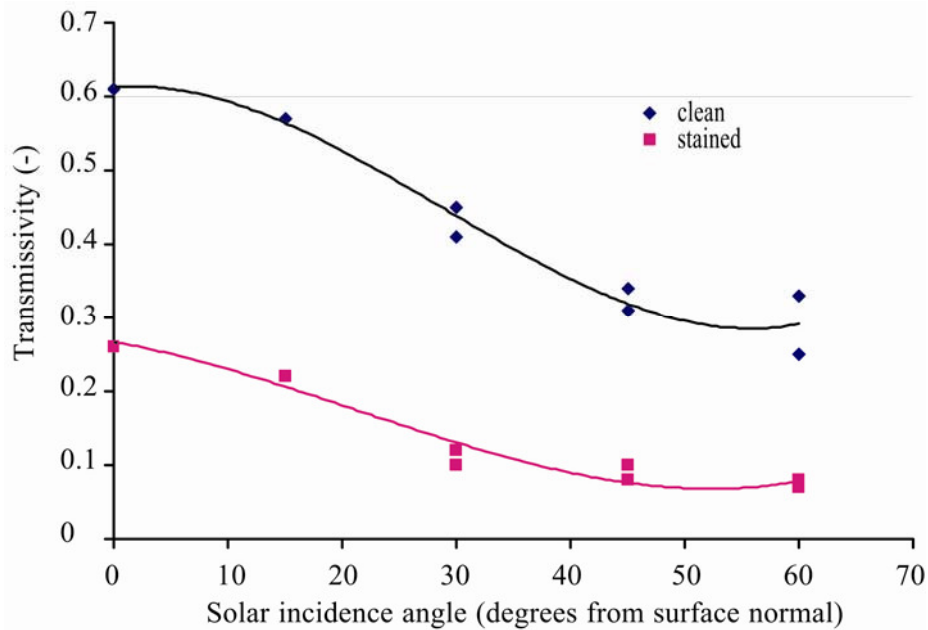


Figure 1: Impact of staining on TI shortwave transmissivity.

Advanced glazings

Advanced glazings provide regulation of energy flow via devices such as multiple panes, inter-pane inert gas filling or vacuum, low emissivity or spectrally selective coatings, optical manipulation (diffusing, re-directing), variable transmissivity, and encapsulated shading. An important factor when adopting advanced glazing is to ensure that the framing does not allow thermal bridges that will compromise overall system performance.

The detailed modelling of the impact of advanced glazings on internal illuminance distribution and glare under different sky conditions depends on the characterisation of transparent and translucent materials (diffusing and non-diffusing) in terms of their response when illuminated by point and diffuse light sources. This requires the

measurement of window normal-normal transmittance (for use with point sources such as the direct solar beam) and hemispherical-hemispherical transmittance (for use with diffusing sources such as the sky). Internal surface finishes also need to be characterised in terms of their reflectance, which will be incident angle dependent in the case of specular surfaces.

In situ measurements

Laboratory testing under standard conditions will be inappropriate where material properties are expected to operate under significantly different conditions in practice. For these cases, *in situ* testing will be required.

A heat flux sensor – a transducer that generates a signal that is proportional to the local heat flux – may be employed to determine the mean value of thermal conductivity of a construction over a given period. Typically the sensor would be embedded within a substrate with a high thermal capacity to minimise the dynamic errors associated with short time constant materials: Figure 5 shows a sensor embedded within a concrete construction block. In this way, the one dimensional heat flow rate can be determined and used to calculate the effective thermal conductivity, k , as a function of the time-averaged temperature difference:

$$k = \frac{Qx}{\Delta T}$$

where Q is the integrated heat flux (W/m^2), ΔT the time-averaged temperature difference across the material (K) and x the material thickness (m).

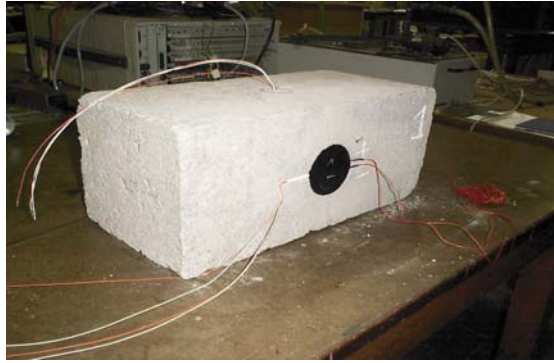


Figure 5: Heat flux sensor embedded within a high density concrete block.

The techniques of pyrometry and photometry may be used to measure, by non-contact means, longwave emissivity and solar optical properties respectively. A pyrometer focuses thermal radiation, q_t , onto a detector, allowing the determination of the surface temperature, θ_s , from the Stefan-Boltzmann law:

$$q_t = \sigma \varepsilon \theta_s^4$$

where σ is a constant and ε the known surface emissivity; if the surface temperature is known, its emissivity can be inferred.

Photometry measurements require lux meters to quantify surface illuminance (lux) and luminance meters to quantify the directional surface luminance (cd/m^2). The Daylight-Europe project (Fontoynt 1999) developed simple procedures for the measurement of material optical properties such as the normal-normal transmittance of non-diffusing glazing under a point light source, the hemispherical-hemispherical transmittance of clear, tinted or diffusing glazing under a diffuse light source, and the reflectance of diffuse or specular surfaces.

Photovoltaic cells

In accordance with European recommendations, manufacturers test their photovoltaic (PV) products under ESTI Test Specification Number 503. In such a test, a module's performance is characterised within an environment where the cell temperatures are maintained at 25°C and the module is exposed to a pulsed irradiance of 1000 W/m². From this test, the current and voltage characteristics are recorded to allow the open circuit voltage, short circuit current, and maximum power point voltage/current to be quantified. Consider Figure 2, which shows a façade-integrated PV component generating electricity and heat; the former is delivered to the building's electricity distribution network, the latter to a heat recovery system.

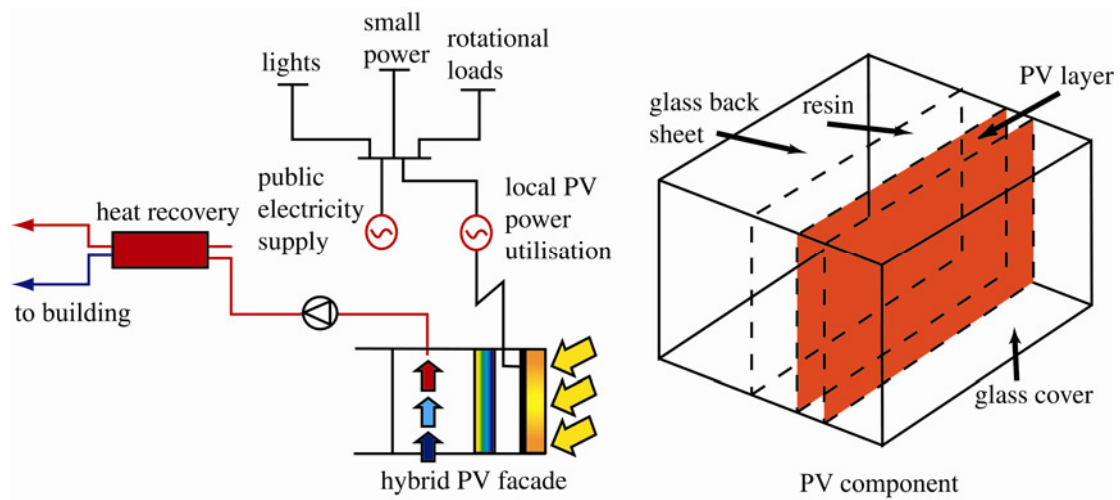


Figure 2: A façade-integrated PV component with local power use.

Solar radiation is transmitted to the surface of the PV layer through the glass cover. A portion of this flux will be converted to electrical energy:

$$\alpha_i = \alpha'_i + q_e$$

where α_i is the irradiation of the PV layer, α'_i the solar radiation absorbed by the PV layer that is converted to heat and q_e the electrical power output. Models exist for the calculation of q_e , such as the one by Buresch (1983):

$$q_e = n.c.p \left[V.I_d \left(\exp \left\langle \frac{eV}{\sigma.d.\theta} \right\rangle - 1 \right) - V.I_L \right]$$

where θ is the temperature (K) of the PV material, V the voltage at maximum power point, I_d the diode current, I_L the light generated current, d the diode factor, n the number of series connected cells, c the number of parallel connected cells, p the number of surface panels, e the electron charge (1.6×10^{-19} Coulombs), and σ the Stefan-Boltzmann constant ($1.38 \times 10^{-23} \text{ W/m}^2\text{K}^4$).

The diode factor and current are given by

$$d = \frac{e(V - V_{oc})}{n.\alpha.\theta_{stc} \log \left(\frac{I_{sc} - I_{mp}}{I_{sc}} \right)}$$

$$I_d = \frac{I_{sc} 2^{\frac{\theta - \theta_{ref}}{\lambda}}}{c.\exp \left(\frac{e.V_{oc}}{n.k.d.\theta_{stc}} - 1 \right)}$$

and the light generated current by

$$I_L = \frac{\alpha' I_{sc}}{c.\alpha'_{stc}}$$

where λ is an empirical factor and θ_{stc} , V_{oc} , I_{sc} , I_{mp} and α'_{stc} are temperature, open circuit voltage, short circuit current, maximum power point current and cell insolation under standard test conditions. These are the parameters that need to be measured in a laboratory test.

Ducted wind turbines

Ideas for wind energy conversion in an urban environment have ranged from the notion of placing wind turbines on roofs, to façade-integrated ducted wind turbines. With reference to Figure 3, when the wind blows at right angles to a tall façade, stagnation will occur at about two-thirds of the total height. Below this level a rolling vortex is formed, above it the air rises to pass over the roof. If the roof is flat, it will separate from the upwind edge, possibly reattaching some distance downstream. A ducted wind turbine (DWT; Grant *et al* 2008) is designed to draw air from the high-pressure region on the upwind face of the building and exhaust it into the low-pressure region above the flat roof. The device will operate efficiently over a 60° range of wind directions, with the ducting serving to dampen any turbulence in the air stream, which can be a significant problem when other buildings are in close proximity.

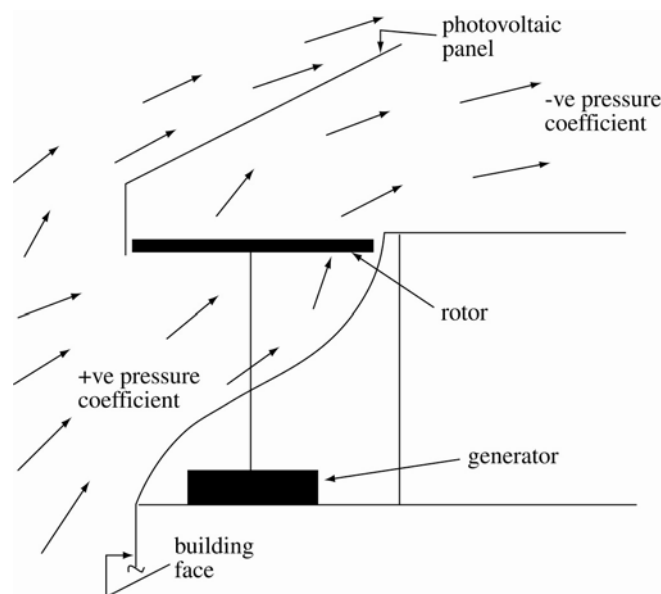


Figure 3: A façade-integrated ducted wind turbine.

The power output, P_w , from a conventional wind turbine may be determined from

$$P_w = 0.5C_p \rho \pi R^2 v^3$$

where v is the wind speed (m/s), R the rotor radius (m), ρ the air density (kg/m³) and C_p a power coefficient that represents the effectiveness of the turbine rotor.

For a given turbine, C_p is a function of the tip speed ratio t_s :

$$t_s = \frac{\omega R}{v}$$

where ω is the angular velocity of the rotor.

Because most conventional grid-connected wind turbines are constrained to turn at constant angular velocity, as the wind speed varies, the value of t_s (and hence C_p) will change. A DWT, being a small unit for autonomous use, is unlikely to be connected to the electrical grid and so can operate in variable-speed mode.

Maintaining a constant value for t_s allows the DWT to operate at a constant and optimum value of C_p .

Combining the previous two equations gives:

$$P_w = T\omega = \frac{0.5C_p \rho \pi R^2 \omega R}{t_s^3} = K\omega^3$$

where K is a constant and the torque T at the rotor shaft follows a quadratic characteristic, $T = K\omega^2$.

In practice it is possible to control the generator to produce a quadratic torque characteristic at the rotor shaft, and so a near-constant value of C_p may be achieved.

This mode of operation can be abandoned in high wind speeds, where it is necessary to limit the power produced. Here, the electrical load on the generator may be increased, reducing the rotor speed, stalling its blades and reducing C_p to the required value. At low wind speeds, say below 5 m/s, the power output will fall as a result of disproportionate mechanical losses and low generator efficiency.

Wind tunnel tests may be used to characterise the change in C_p over the operational range: Figure 4 shows measured power output, P_m , and C_p against wind speed from such a test. The variation in C_p is determined from

$$\frac{P_m}{P_i}$$

where P_i is the ideal power output given by

$$P_i = 0.5\rho Av^3$$

where ρ is the air density, A the swept rotor area and v the wind speed.

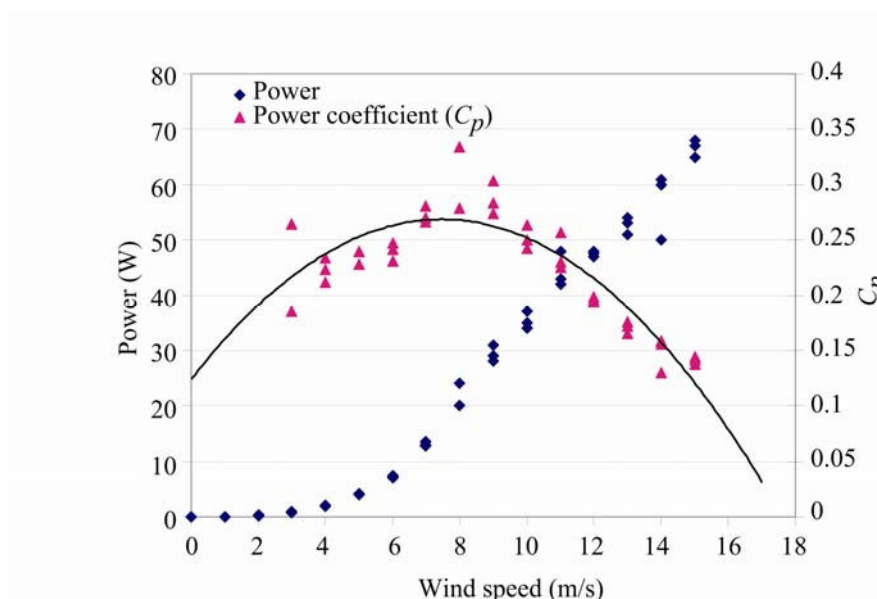


Figure 4: Monitored power output and C_p value for a ducted wind turbine.

Integrated performance rating

At the core of all simulation programs is a detailed mathematical representation of the heat transfer processes occurring within the building. At its most general, the approach taken is to transform the real system to a discretised equivalent and to represent each part by conservation equations relating to energy, mass and momentum exchanges. The problem then becomes one of estimating the temporal evolution of the parameters comprising the coefficients of these equations and arranging for whole-system equation solution under the influence of time varying boundary conditions.

It is widely accepted that integrated modelling defines a new best practice approach to energy systems design because it allows designers to address important new challenges such as the linking of energy, the environment, comfort and health. In use, the approach requires the gradual evolution of a problem's description, with performance outputs becoming available at discrete stages as the design detail improves. The design team is then free to terminate model building when the objectives have been achieved.

Models such as those described in the preceding section, along with their related parameter values established by laboratory or *in situ* testing, and as summarised in Table 1, have been encapsulated within building performance simulation programs so that advanced façade options may be readily appraised. The approach is accurate, in that the various energy transport mechanisms are explicitly represented, and rational in that performance is quantified in terms of a range of relevant criteria addressing technical, environmental and comfort issues. Figure 6, for example, shows an

Integrated Performance View (IPV; Prazeres and Clarke 2005) as output by one contemporary building performance simulator, ESP-r (Clarke 2001). An IPV reports on issues such as seasonal energy demand, thermal/visual comfort, daylight utilisation, renewable energy contributions and environmental impact in relation to global warming, atmospheric acidification and ozone generation potentials.

Table 1: Experimentally derived parameters as required by advanced façade modelling and simulation.

Component	Parameters
Material bulk properties	conductivity, density, specific heat capacity
Surface finish	emissivity, absorptivity, reflectivity
Glazing	angular transmissivity, reflectivity and absorptivity
Transparent insulation	maintenance impact on solar transmissivity
Photovoltaic cells	open circuit voltage, short circuit current, maximum power point current
Ducted wind turbines	power coefficient

The following section demonstrated the application of the integrated modelling technique to the design of an advanced façade in a manner that gives rise to a self referential benchmarking technique.

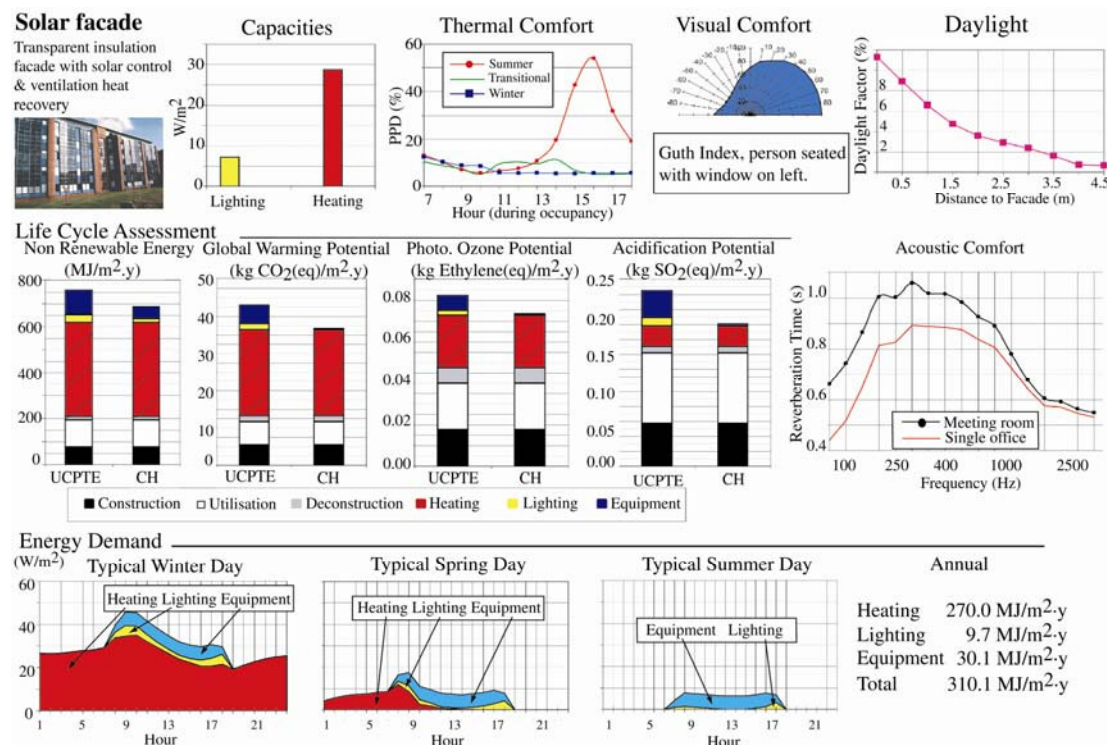


Figure 6: An integrated view of building performance.

Application in practice

To illustrate the integrated modelling approach to advanced façade design, this section summarises two projects: the encapsulation of transparent insulation material and solar control devices within the façade of a new student residence located at the University of Strathclyde, and the encapsulation of all the above mentioned technologies within a refurbished building in Glasgow.

Case Study 1: Student residences

This project (Roddick *et al* 1993) entailed the development of accommodation for 376 students and included pre-design modelling and post-occupancy monitoring. As depicted in Figure 7, the development incorporated a 1040 m² solar façade containing polycarbonate honeycomb transparent insulation and an automated solar shading mechanism. Figure 7 also shows the façade cross section to summarise the operational principle.

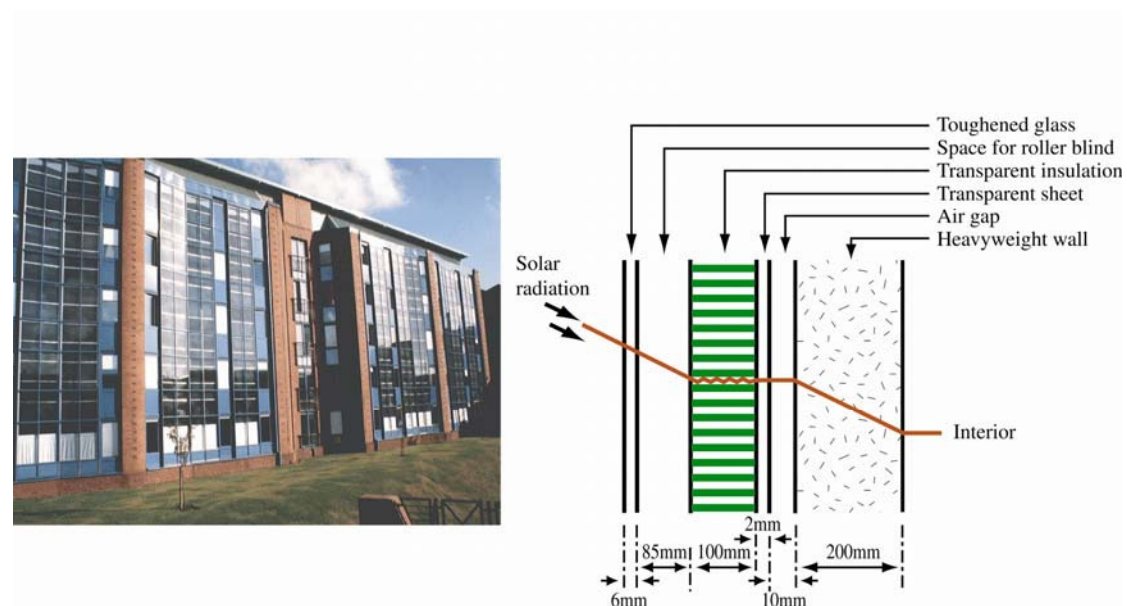


Figure 7: Solar façade at the University of Strathclyde student residences.

Heat flux sensors embedded in the façade indicated a dark U-value of $0.6 \text{ W/m}^2\text{K}$ with the shading device open and $0.48 \text{ W/m}^2\text{K}$ with the device closed. Over the heating season, more energy enters than leaves the façade; hence an overall U-value of $-0.08 \text{ W/m}^2\text{K}$. The Normalised Performance Indicator (NPI) value of 168 $\text{kWh/m}^2\text{.yr}$ represents a 40% improvement on the ‘Good’ classification for a building of this type.

Post occupancy monitoring quantified the contribution to the heating load from the façade as 293 MWh/year, while a survey showed that 91% of the occupants were ‘satisfied’ or ‘very satisfied’ with the internal environment – the average room temperature in winter was 20-24°C.

Case Study 2: Commercial refurbishment

This project (Clarke *et al* 2000) was undertaken as part of the renovation of a former Glasgow Herald building – a notable Charles Rennie Mackintosh design – to create ‘The Lighthouse’, Scotland's Centre for Architecture and Design (as depicted in Figure 9). Modelling and simulation was used to search for façade-oriented technologies that effected a favourable match between the supply from façade-integrated renewable energy components and building electricity and thermal demands. The outcome from this search included:

- advanced glazings to minimise heat loss without significantly reducing daylight penetration;
- a façade with transparent insulation and integral solar control blind to translate solar energy over time to offset heating requirements;

- dynamic indoor temperature and illuminance set-point adjustment;
- an array of ducted wind turbines (DWT) to meet a portion of the power demands during the winter and transitional seasons;
- a PV array to meet a portion of the power demand during the transitional and summer seasons (this array was subsequently incorporated within the spoiler of the DWT);
- a hybrid PV façade to meet a portion of the power and heat demands during the transitional and summer seasons; and
- a battery storage system to meet the temporal mismatch between the demand and supply.

Figure 8 shows the cumulative impacts of the demand reduction measures: a 68% reduction in annual energy demand (corresponding to a 58% reduction in heating and an 80% reduction in lighting). Significantly, the final demand profiles are better matched to the output from the locally deployed renewable energy (RE) systems.

As shown in Figure 9, the hybrid PV component was subsequently incorporated within the south-facing façade, while the DWTs were mounted at the top edges of the south- and west-facing façades. The predicted power outputs from the two RE technologies are also shown superimposed on the most favourable demand profile. Because of the residual temporal mismatch, the RE supply could be used to meet approximately 65% of the total demand. This value would fall to approximately 20% for the case where the demand reshaping measures were not firstly applied.

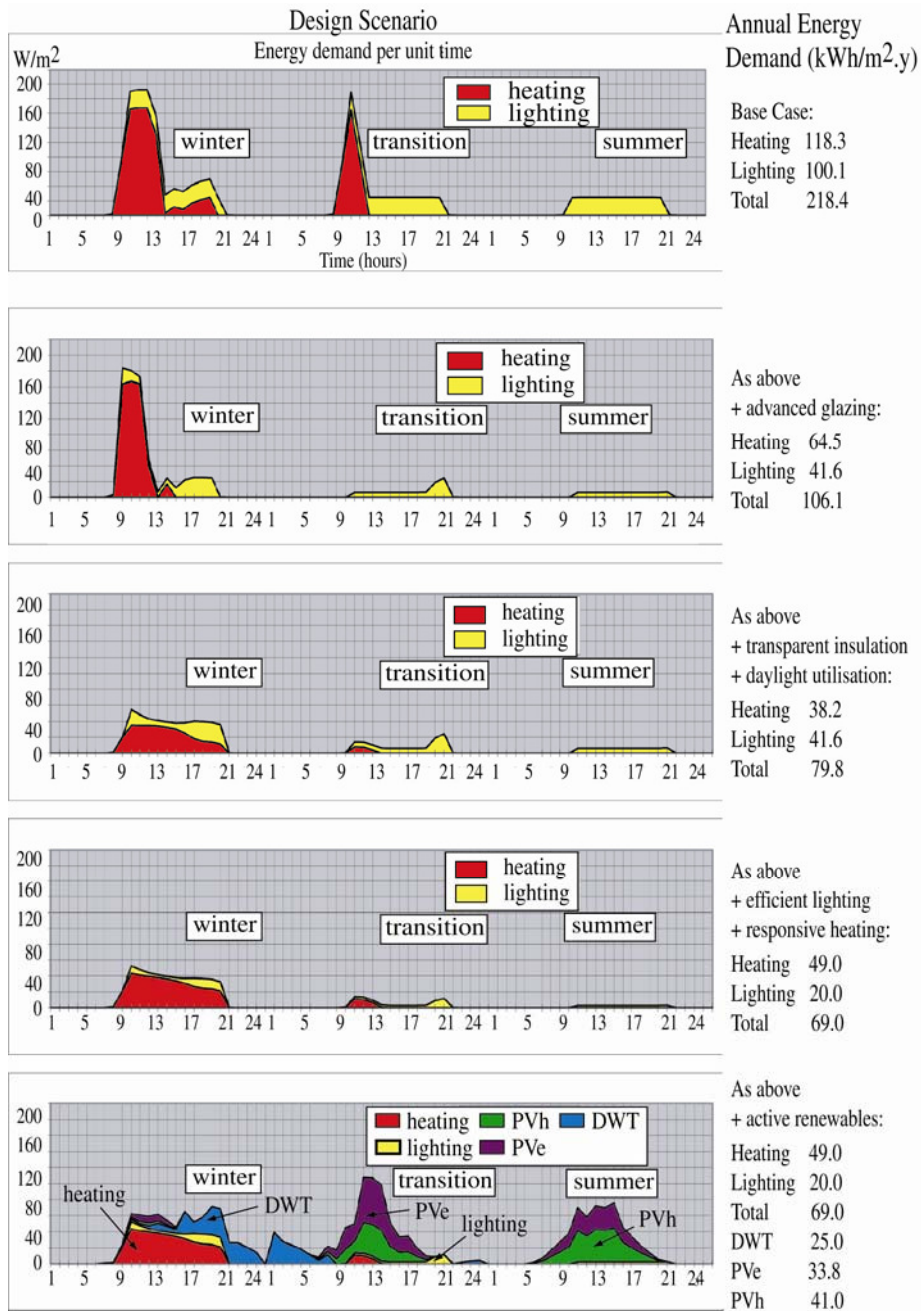


Figure 8: Impact of progressive deployment of demand reshaping measures.

Benchmarking façade performance

While there is a paucity of information on the performance of advanced façades that incorporate technology mixes as above, there is much in the literature on building energy benchmarking in general (e.g. CIBSE 2009, Carbon Trust 2009) and the energy performance of specific façade designs (e.g. de Matos and Duarte 2007). In

addition, procedures have been developed to assess the non-energy performance of facades related to the risk of defect occurrence (e.g. Chew and de Silva 2004).

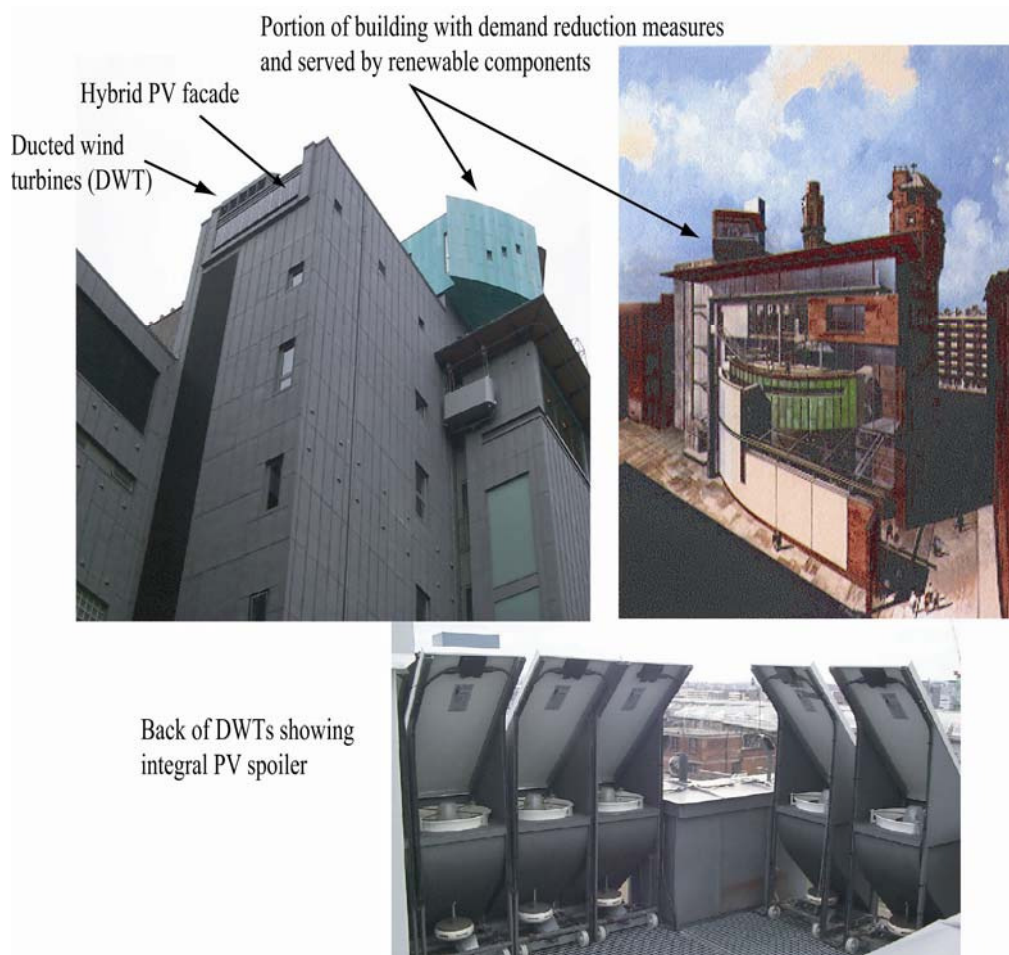


Figure 9: Embedded RE systems in The Lighthouse Building, Glasgow.

One way to assess the energy benefit that may accrue from the different possible façade technologies is to use simulation to quantify the benefits of possible combinations. This approach was employed in the case studies reported above. In the case of the Lighthouse building, the initial predicted performance of 218 kWh/m².yr for heating and lighting could be improved to around 106 kWh/m².yr by the deployment of advanced glazing for heat loss reduction, to around 80 kWh/m².yr by the additional deployment of TIM and daylight capture/utilisation, and to around 60

kWh/m².y by the adoption of smart heating/lighting system control. The integration of PV and DWT technologies, which were made viable by the reshaped demand profiles, resulted in the production of around 100 kWh/m².yr, although not all of this was utilisable because of the temporal mismatch.

In the case of the student residences, the solar façade resulted in a 40% reduction in the NPI – from 280 kWh/m².yr to 168 kWh/m².yr.

Arriving at such low energy façade solutions requires a procedure for systematically analysing the different demand/supply options. This is made possible within the modelling and simulation approach by adherence to a *Performance Assessment Method* that explores the impact of the different possible technologies when deployed separately and together. In the case of the Lighthouse building, for example, the cumulative impacts shown in Figure 8 comprise only a sub-set of those actually considered but discarded for a variety of reasons specific to the project (e.g. cost). The important point is that the initial design must not be constrained by the incorporation of particular low energy features. Rather, these features should be systematically added to the initial, unconstrained design hypothesis so that the impact of each feature may be judged in a relative manner and suitable outcomes retained. Clearly, the actual features considered will change with time as existing technologies become cost-effective and new technologies emerge.

Further information

Selkowitz (2001) has given a useful overview of the issues underpinning advanced façade design and perhaps the most definitive source of information on the concepts,

technologies and tools for high performance building façade solutions is the resource base maintained by the Environmental Energy Technologies Division at the Lawrence Berkeley National Laboratory (see <http://lowenergyfacades.lbl.gov/resources.html>).

Another useful Web site on the topic is maintained at

<http://www.energy.soton.ac.uk/buildings/facades.html> and state-of-the-art viewpoints are available as part of recent conference proceedings (e.g. Facade Engineering 2009).

References

- Buresch M (1983) *Photovoltaic energy systems - design and installation*, McGraw-Hill, New York.
- Clarke J A, Johnstone C M, Macdonald I A, French P, Gillan S, Glover C, Tatton D, Devlin J and Mann R (2000) 'The Deployment of Photovoltaic Components Within the Lighthouse Building in Glasgow', *Proc. 16th European Photovoltaic Solar Energy Conf.*, Glasgow.
- Carbon Trust (2009)
www.carbontrust.co.uk/energy/assessyourorganisation/benchmarking.htm.
- Chew M Y L and De Silva N (2004) 'Factorial Method for Performance Assessment of Building Facades', *Journal of Construction Engineering and Management*, 130(4).
- CIBSE (2009) Various Energy Benchmark publications of the Chartered Institution of Building Services Engineers (www.cibse.org).
- Clarke J A (2001) *Energy Simulation in Building Design (2nd Edn)*, Butterworth-Heinemann, ISBN 0 7506 5082 6.
- Clarke J A and Yaneske P (2009) 'A Rational Approach to the Harmonisation of the Thermal Properties of Building Materials', *Building and Environment*, 44, pp2046-2055.

de Matos M and Duarte R (2007) 'A comparison between energy performance of one double skin facade buildings studied sample and office buildings benchmarks in Europe (sic)', *Proc. 2nd PALENC Conf. and 28th AIVC Conf. on Building Low Energy Cooling and Advanced Ventilation Technologies in the 21st Century*, Crete, pp253–257.

Façade Engineering (2009) *Proc. façade engineering conference: benchmarking performance and driving innovation in modern façade design*,
www.emapconferences.co.uk/facadeengineering/programme/index.jsp.

Fontoynt M (Ed) (1999) *Daylight Performance of Buildings*, James & James, ISBN 1-873936-87-7.

Grant A D, Johnstone C M and Kelly N (2008) 'Urban wind energy conversion: The potential of ducted wind turbines', *Renewable Energy*, 33(6), ISSN: 0960-1481.

Imbabi M S and Peacock A (2004) 'Allowing Buildings to Breathe', *Renewable Energy*, pp85–95, ISSN/ISBN: 0960-1481.

IEA (2002) 'Photovoltaics/thermal solar energy systems: Status of the technology and roadmap for future development', *Task 7 Final Report*, International Energy Agency PVPS T7-10.

Hutchins M (1998) 'Advanced glazings: a status report', *Sunworld*, 22(1), pp5–11, ISSN 0149-1938.

Kumaran M K (1996) 'Hygrothermal Properties of Building Materials', *Final Report for Task 3*, IEA Annex 24 (Heat Air and Moisture Transfer in Insulated Envelope Parts), International Energy Agency.

Künzel H M and Kiessl K (1997) 'Calculation of Heat and Moisture Transfer in Exposed Building Components', *Journal of Heat Mass Transfer*, 40(1), pp.159–167.

- Loncour X, Deneyer A, Blasco M, Flamant G, and Wouters P (2004) *Ventilated double façades – Classification & illustration of façade concepts*, Belgian Building Research Institute.
- Prazeres L and Clarke J A (2005) 'Qualitative analysis of the usefulness of perceptualisation techniques in communicating building simulation outputs', *Proc. Building Simulation '05*, Montreal, International Building Performance Simulation Association.
- Roddick G, Twidell J W and Johnstone C M (1993) Final Report for Contract SE/324/87, European Commission.
- Rode C and Grau K (2008) 'Moisture Buffering and its Consequence in Whole Building Hygrothermal Modeling', *J. Building Physics*, 31(4), pp333–360.
- Selkowitz S E (2001) 'Integrating advanced facades into high performance buildings' *Paper LBNL-47948*, Lawrence Berkeley National Laboratory.
- Selkowitz S, Aschehoug O and Lee E S (2003) 'Advanced Interactive Facades – Critical Elements for Future Green Buildings?', *Proc. GreenBuild*, Lawrence Berkeley National Laboratory.
- Wittwer V and Platzer W (2000) 'Transparent thermal insulation materials and systems: State of the art and potential for the future', *J. High temperatures, high pressures*, 32(2) pp143–158.